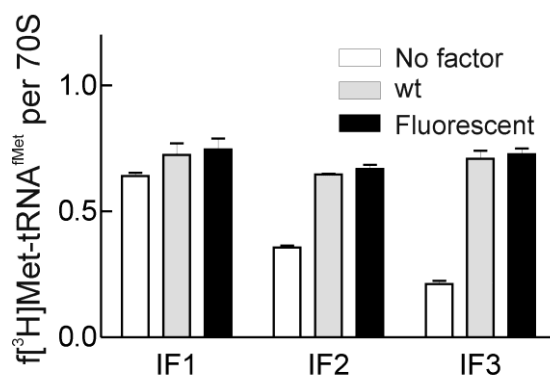
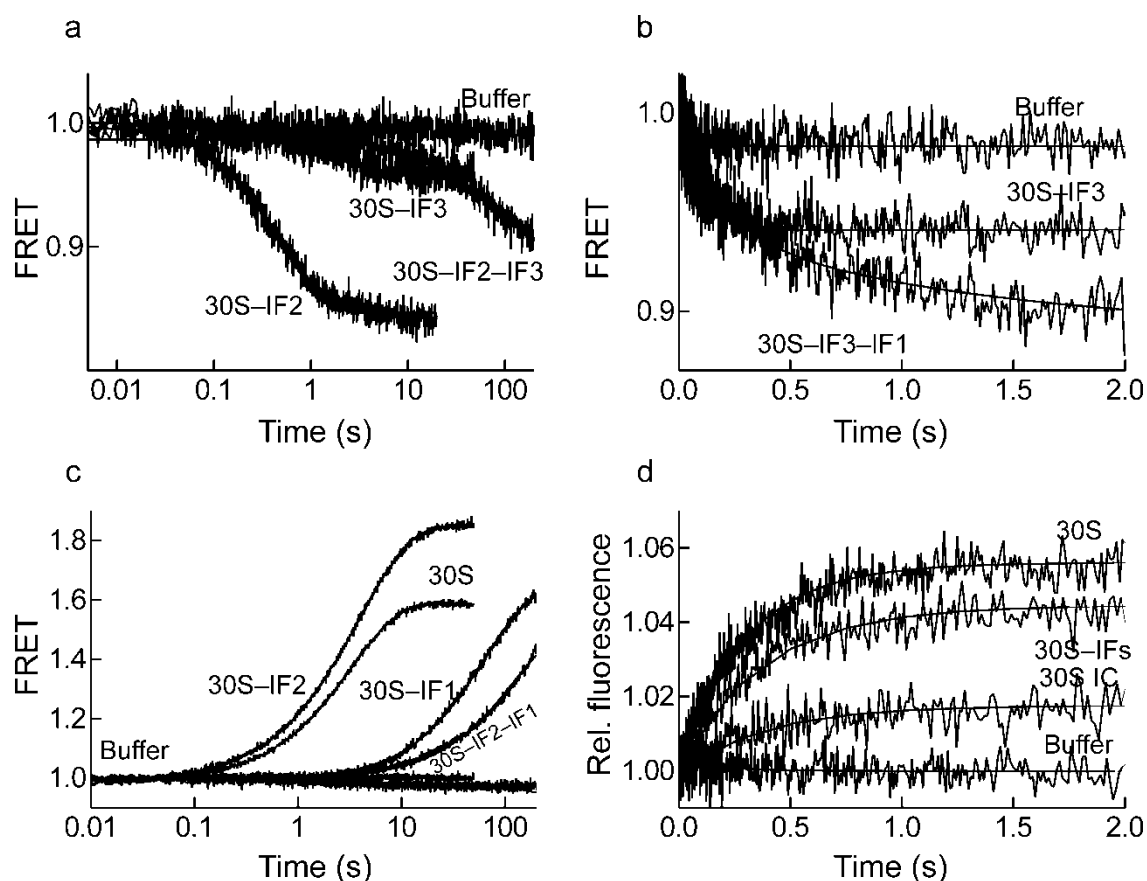


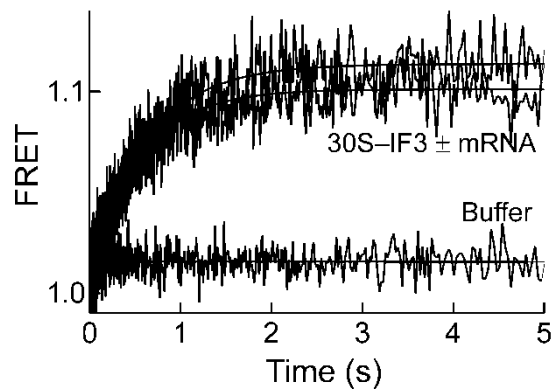
## Supplementary Results



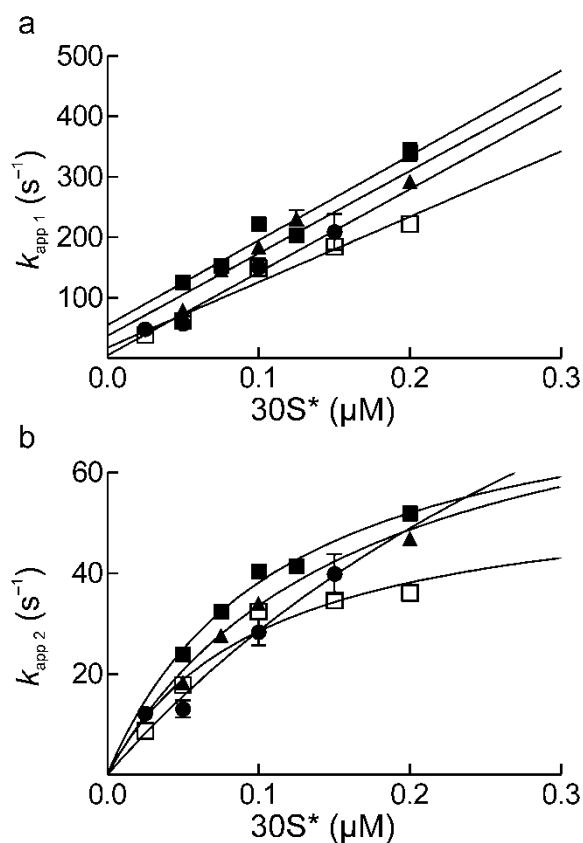
**Supplementary Figure 1. Functional activity of fluorescent derivatives of initiation factors.** 70S IC were formed with  $f[{}^3\text{H}]\text{Met-tRNA}^{\text{fMet}}$  and mRNA (m022) in the absence of the respective factor (white bars), in the presence of the respective unmodified (wt) factor (grey bars), or with fluorescence-labeled mutant initiation factor (black bars). The extent of complex formation was determined by nitrocellulose filtration.



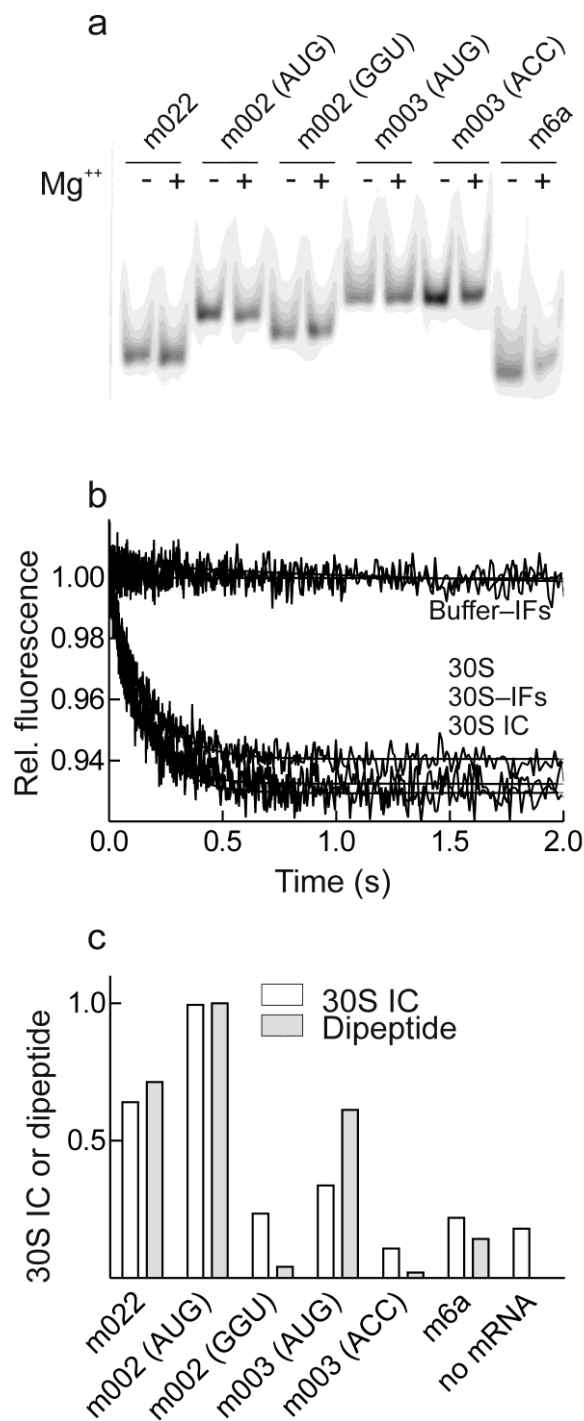
**Supplementary Figure 2. Time courses of IF and mRNA dissociation.** (a) Chase of IF1 from 30S complexes with IF2 or IF3 or IF2 + IF3. Complexes were formed using 30S subunits (0.05  $\mu\text{M}$ ), IF1<sub>4</sub>(Alx555) (0.5  $\mu\text{M}$ ), IF3<sub>166</sub>(Alx488) (0.06  $\mu\text{M}$ ), IF2 (0.15  $\mu\text{M}$ ) or IF2<sub>757</sub>(Alx488) (0.11  $\mu\text{M}$ ), GTP (0.25 mM), as indicated; the dissociation was initiated by the addition of unlabeled IF1 (5  $\mu\text{M}$ ). (b) Chase of IF2<sub>599</sub>(Atto465) from various 30S complexes was initiated by the addition of unlabeled IF2 (1.5  $\mu\text{M}$ ). 30S complexes (0.05  $\mu\text{M}$ ) were prepared with IF2<sub>599</sub>(Atto465) (0.11  $\mu\text{M}$ ), GTP (0.25 mM) in the absence or presence of IF1 (1  $\mu\text{M}$ ), IF3<sub>166</sub>(Alx555) (0.1  $\mu\text{M}$ ), mRNA (0.4  $\mu\text{M}$ ). (c) Chase of IF3. Complexes were formed by incubating 30S subunits (0.1  $\mu\text{M}$ ) with IF3<sub>166</sub>(Alx488) (0.01  $\mu\text{M}$ ), and mRNA(AttoQ) (0.4  $\mu\text{M}$ ) and where indicated IF1 (1  $\mu\text{M}$ ), IF2 (0.3  $\mu\text{M}$ ) with GTP (0.25 mM), and fMet-tRNA<sup>fMet</sup> (0.3  $\mu\text{M}$ ). The dissociation was initiated by addition of unlabeled IF3 (1  $\mu\text{M}$ ) to the 30S complex containing the FRET pair. (d) Chase of mRNA(Atto488) from 30S·mRNA complexes by excess of unlabeled mRNA. The dissociation of the fluorescent mRNA from the complexes (0.05  $\mu\text{M}$ ) was initiated by addition of unlabeled mRNA (1.5  $\mu\text{M}$ ).



**Supplementary Figure 3. IF1 binding to 30S:IF3 complex in the presence or absence of mRNA.** IF1(A1x555) (0.15  $\mu\text{M}$ ) was rapidly mixed with 30S subunits (0.05  $\mu\text{M}$ ) in complex with IF3(A1x488) (0.06  $\mu\text{M}$ ) in the absence or presence of mRNA (0.3  $\mu\text{M}$ ). Lower line, control without ribosomes.



**Supplementary Figure 4. Concentration dependence of  $k_{app1}$  and  $k_{app2}$  values of IF3 binding to 30S complexes. (a) Linear dependence of  $k_{app1}$  values. (b) Hyperbolic dependence of  $k_{app2}$  values. The estimations of the elemental rate constants were used as initial parameters for global fitting. Experimental conditions are indicated in Fig. 4. Symbols: (■) 30S subunit; (●), with IF1; (▲) with IF2; (□) with IF1 and IF2.**



**Supplementary Figure 5. Binding, conformation and functional activities of mRNAs. (a)**

Mobility of mRNAs on a non-denaturing PAGE. 10 pmol of each fluorescent mRNA were loaded onto the gel after renaturation in the presence or absence of 7 mM magnesium acetate. Gels were run for 2.5 h at 4°C in TBE buffer and scanned using F7000 scanner with a fluorescence filter for Cy2 (GE Healthcare). **(b)** Time courses of mRNA(m022) binding to vacant 30S subunits, 30S with IF1, IF2, and IF3 (30S·IFs), or to the 30S·IFs·fMet-tRNA<sup>fMet</sup>

complex; topmost curve, control without ribosomes. Complex formation was monitored by the fluorescence change of Atto488 attached to position +12 of the mRNA. In the presence of the highly structured m6a mRNA<sup>1</sup>, no fluorescence intensity change was recorded (not shown) indicating that the signal observed for the other mRNAs originate from the association of single stranded segments of the constructs<sup>1</sup>. (c) 30S IC and dipeptide formation with mRNAs used in this study. The amount of [<sup>3</sup>H]Met-tRNA<sup>fMet</sup> bound to the 30S subunits was measured by nitrocellulose filtration and liquid scintillation counting. The relative values indicate efficiencies of fMet-tRNA<sup>fMet</sup> recruitment for each mRNA normalized by the efficiency obtained when m002 mRNA was used, typically between 80-100%. Dipeptide formation was measured after addition of 50S subunits, EF-Tu, GTP, [<sup>14</sup>C]Phe-tRNA<sup>Phe</sup>, phosphoenol pyruvate, and pyruvate kinase to the 30S IC as described<sup>2</sup>. Relative efficiency values were calculated as for 30S IC formation measurements.

**Supplementary Table 1. List of fluorescent reporters used in this work**

<b>Component</b>	<b>Modified residue</b>	<b>Dye</b>	<b>Comments</b>	<b>Figure</b>
IF1 <sub>4</sub> (Alx555)	D4C	Alexa 555	FRET acceptor for IF3 <sub>166</sub> (Alx488), IF2 <sub>757</sub> (Alx488)	Fig. 2, 6e, S2
IF2 <sub>757</sub> (Alx488)	C599S/V757C	Alexa 488	FRET donor for IF3 <sub>166</sub> (Alx555), IF1 <sub>4</sub> (Alx555)	Fig. 2, S2
IF2 <sub>599</sub> (Atto465)	<i>wt</i> Cys599	Atto 465	FRET donor for IF3 <sub>166</sub> (Alx555), IF1 <sub>4</sub> (Alx555)	Fig. 3, 6e
IF3 <sub>166</sub> (Alx488)	C65S/E166C	Alexa 488	FRET donor for IF1 <sub>4</sub> (Alx555), tRNA <sup>Phe</sup> (QSY), mRNA (AttoQ)	Fig. 2, 4, 5, 6e, S2, S3, S4
IF3 <sub>166</sub> (Alx555)	C65S/E166C	Alexa 555	FRET acceptor for IF2 <sub>757</sub> (Alx488), IF2 <sub>599</sub> (Atto465), fMet-tRNA <sup>fMet</sup> (Flu)	Fig. 3, S2
tRNA <sup>Phe</sup> (QSY)	Thio-U8	QSY-35	FRET acceptor for IF3 <sub>166</sub> (Alx488)	Fig. 5
mRNA(AttoQ)	5' end	Atto 540Q	FRET acceptor for IF3 <sub>166</sub> (Alx488)	Fig. 4, 6e S2
mRNA(Atto488)	3' end (+12)	Atto 488	Fluorescence change	Fig. 6, S3, S4, S5

**Supplementary Table 2. Dissociation rate constants of IF2 from 30S complexes.**

<b>IF2</b>	<b><math>k_{\text{off}}^{\text{a}}</math></b>
<b>Complex</b>	<b><math>\text{s}^{-1}</math></b>
30S–IF3	$15 \pm 0.7$
30S–IF3–mRNA	$12 \pm 0.6$
30S–IF1–IF3	$1 \pm 0.1$
30S–IF1–IF3–mRNA	$2 \pm 0.1$
30S IC, no IF3	$0.05 \pm 0.005$
30S IC, no IF1	$0.17 \pm 0.01$
30S IC	$0.04 \pm 0.005$

<sup>a</sup> Dissociation rate constant determined in chase experiments (**Fig. 3d**). To form 30S IC, m022 mRNA was used.



**Supplementary Table 3. Association and dissociation rate constants of mRNA binding to 30S complexes.**

		Vacant 30S		30S-IFs		30S IC	
20 °C	$T_m$	$k_{on}^a$	$k_{off}^b$	$k_{on}^c$	$k_{off}^b$	$k_{on}^c$	$k_{off}^b$
mRNA	°C	$\mu M^{-1}s^{-1}$	$s^{-1}$	$\mu M^{-1}s^{-1}$	$s^{-1}$	$\mu M^{-1}s^{-1}$	$s^{-1}$
<b>m022</b>	50	15 ± 2	3 ± 0.1	36 ± 1	2.5 ± 0.1	48 ± 1	n.d.
<b>m002(AUG)</b>	41	43 ± 6	0.05 ± 0.005	40 ± 1	0.06 ± 0.005	38 ± 1	n.d.
<b>m002(GGU)</b>	49	54 ± 1	0.05 ± 0.005	46 ± 1	0.04 ± 0.005	45 ± 1	0.04 ± 0.01
<b>m003(AUG)</b>	22	49 ± 3	0.06 ± 0.005	84 ± 1	0.06 ± 0.005	95 ± 1	0.09 ± 0.001
<b>m003(ACC)</b>	18	59 ± 4	0.05 ± 0.005	118 ± 2	0.05 ± 0.005	112 ± 2	0.05 ± 0.001
<b>37 °C</b>		$k_{on}^a$	$k_{off}^b$				
mRNA		$\mu M^{-1}s^{-1}$	$s^{-1}$				
<b>m022</b>		36 ± 4	13 ± 0.1				
<b>m002(AUG)</b>		110 ± 7	1.2 ± 0.05				
<b>m002(GGU)</b>		94 ± 11	1 ± 0.1				
<b>m003(AUG)</b>		95 ± 6	2.8 ± 0.02				

<sup>a</sup> Association rate constants determined from the slope of the linear concentration dependence of  $k_{app}$  (for a one-step mechanism).

<sup>b</sup> Dissociation rate constant determined in chase experiments. n.d., not detectable (too slow).

<sup>c</sup> Association rate constants estimated from  $k_{app} = k_{on} \times [30S] + k_{off}$  for a one-step mechanism.

## References

1. Studer, S.M. & Joseph, S. Unfolding of mRNA secondary structure by the bacterial translation initiation complex. *Mol. Cell* **22**, 105-115 (2006).
2. Milon, P. et al. The nucleotide-binding site of bacterial translation initiation factor 2 (IF2) as a metabolic sensor. *Proc. Natl. Acad. Sci. USA* **103**, 13962-13967 (2006).